Nitride tuning of transition metal perovskites

Amparo Fuertes

COLLECTIONS

Paper published as part of the special topic on New Perspectives on Emerging Advanced Materials for Sustainability

Note: This paper is part of the Special Issue on New Perspectives on Emerging Advanced Materials for Sustainability.

View Online

Export Citation

CrossMark

ARTICLES YOU MAY BE INTERESTED IN

ORDER PRINT EDITION

AIP Conference Proceedings
The 18th International Conference on Positron Annihilation

Nitride tuning of transition metal perovskites

View Online   Export Citation   CrossMark

Amparo Fuertes[a]

AFFILIATIONS

Institut de Ciència de Materials de Barcelona (ICMAB-CSIC), Campus UAB, 08193 Bellaterra, Spain

Note: This paper is part of the Special Issue on New Perspectives on Emerging Advanced Materials for Sustainability.
[a]Author to whom correspondence should be addressed: amparo.fuertes@icmab.es

ABSTRACT

Transition metal perovskite oxynitrides are emergent materials for applications as visible light-active photocatalysts for water splitting and CO_2 reduction and as thermoelectric, dielectric, and magnetic materials. They have been reported for early transition metals Ti, Zr, Hf, V, Nb, Ta, Cr, Mo, and W in the B sites and alkaline earth or rare earth metals in the A sites. Nitrogen is less electronegative and more polarizable than oxygen, and nitride is more charged than oxide. As a consequence, the introduction of nitride in an oxidic perovskite has important effects on the covalency of bonds, the energy of electronic levels, and the valence states of the cations. This work discusses fundamental and recent developments of perovskite oxynitrides of transition metals of groups 4, 5, and 6 as photocatalytic and electronic materials, focusing on the important aspects of synthetic methodologies, crystal structures, and anion ordering, in connection with the observed physical and chemical properties. Some examples of compounds with late transition metals and complex structures such as layered and double perovskites are also discussed.

I. INTRODUCTION

Transition metal perovskite oxides are of permanent interest because they show innumerable important properties and applications. Their chemical diversity may be expanded by modifying the anion composition with the introduction of nitride that shows electronic and crystal chemical characteristics close to oxide.[1] Nitrogen is less electronegative and more polarizable than oxygen, and nitride is more charged than oxide. These crucial differences between the two anions are the important factors affecting the chemical and physical properties of perovskite oxynitrides $ABO_{3-x}N_x$ (A = alkaline earth or rare earth metal; B = transition metal). They have been investigated for several important applications, more intensively as water splitting photocatalysts active under visible light for hydrogen generation[2] and as materials with high dielectric constants.[3] Perovskite oxynitrides also show remarkable applications as non-toxic pigments[4] and as thermoelectric,[5] magnetic,[6] and ferroelectric materials.[7,8]

When substituting oxide in a semiconductor, nitride introduces 2p states at the top of the valence band, decreasing the bandgap and affecting, for instance, the photocatalytic activity that shifts

to the visible light.[9] The higher charge of N^{3-} increases the ionic polarizability and the dielectric constant. The possibility of formation of permanent electric dipoles[8] is affected by the order of the two anions,[10–13] which also has an impact on the bandgap[14] and other relevant properties. To compensate the −3 charge of nitride, the oxidation states of the transition metals have to be high. They should be stable in the reducing conditions under NH_3 or at high temperatures under N_2 flow that are used for the synthesis of oxynitrides. These two requirements have directed the majority of explored compositions of perovskite oxynitrides to early transition metals from groups 4, 5, and 6, which have stable high valence states and show relative low electronegativities.

The most common method for the synthesis of perovskite oxynitrides is ammonolysis of ternary oxide precursors.[15,16] The direct solid state reaction under NH_3 between individual metal oxides or salts has been used for perovskites containing alkaline earth cations, and also high temperature reactions between nitrides, oxynitrides, and oxides under N_2 have been performed.[17]

Research in perovskite oxynitrides was initiated in the 1970s by Marchand and co-workers, who reported the first example of

layered Nd_2AlO_3N[18] with K_2NiF_4-type structure and, later, the alka-line earth tantalum and niobium perovskites $BaTaO_2N$, $BaNbO_2N$, $SrTaO_2N$, and $CaTaO_2N$.[15,19] The interest in the field was stim-ulated in 2000 with the publication in *Nature* by Jansen and Letschert[4] of new non-toxic red-yellow pigments in the solid solution $Ca_{1-x}La_xTaO_{2-x}N_{1+x}$ and, later, with other early reports from different groups of new compounds with additional appli-cations.[3,20–22] Research during the first decade after these ini-tial reports was reviewed by Ebbinghaus *et al.* in 2010[23] and Fuertes in 2012.[24] This perspective aims at giving a present overview of the reported compounds in the three groups of tran-sition metals, identifying new challenges, and focusing on rele-vant aspects and progress in the synthesis pathways, important structural features such as anion order, and chemical and physical properties.

II. TITANIUM, ZIRCONIUM, AND HAFNIUM COMPOUNDS

A. Titanium

Within the group 4, the titanium compounds are the most investigated because of their photocatalytic activity and dielec-tric properties. $LaTiO_2N$ and $NdTiO_2N$ were first prepared by Marchand *et al.* by ammonolysis at $900\,^{\circ}C$ of $Ln_2Ti_2O_7$ (Ln = La, Nd).[25] For Ln = La, another method treating this oxide and urea under N_2 has also been suggested.[26] The crystal structure of the lanthanum compound was initially reported to be triclinic I-1[17] from the refinement of neutron powder diffraction data. Further investigation on a highly crystalline sample prepared by a flux method indicated the orthorhombic symmetry Imma, using elec-tron diffraction and refinement from synchrotron and neutron pow-der diffraction data.[27] The distribution of nitride and oxide was found totally disordered in the two studies, and more recently as partially ordered[28] with occupancies in agreement with a *cis* con-figuration of nitrides as suggested for $SrTaO_2N$, $SrNbO_2N$, and other perovskite oxynitrides[11,29,30] (Fig. 1). Recent density func-tional theory (DFT) calculations have indicated that whereas a N-*cis* configuration is more stable in bulk $LaTiO_2N$, a non-polar *trans* arrangement of nitrides is preferred at the (001) surface of this perovskite.[31]

$LaTiO_2N$ with a bandgap of 2.1 eV and an absorption edge of 600 nm is one of the most studied perovskite oxynitrides since the first report by Domen *et al.* on its ability to split water under visible light in the presence of sacrificial agents.[32–34] It showed a low apparent quantum yield that was improved significantly using CoO_x as co-catalyst.[35,36] The photocatalytic activity improved in samples obtained by treatment of $La_2Ti_2O_7$ crystals in NH_3 using different fluxes.[37] $LaTiO_2N$ is also active as photocatalyst under visible light for the reduction of CO_2 into CH_4 in the presence of H_2O.[38] As a dielectric material, it has been investigated in the form of ceramics and thin films. The films were grown by radio frequency reactive magnetron sputtering on $Pt/Si/SiO_2/Si$[39] or $Nb:SrTiO_3$[40] substrates using $LaTiO_2N$ or $La_2Ti_2O_7$ targets, respectively. The measured dielectric constant ε_r was 750 for a ceramic sample,[28] whereas it was 325 for a thin film deposited on Nb–$SrTiO_3$.[40]
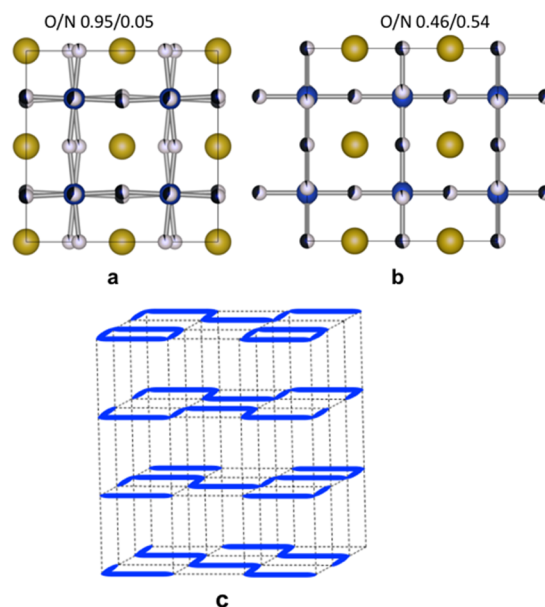

FIG. 1. Crystal structure of the perovskite $SrTaO_2N$[29] projected along (a) [001] and (b) [010] directions of the superstructure $2a_p \times 2a_p \times 2a_p$ of the perovskite sub-cell (of parameter a_p) showing N/O occupancies determined by neutron diffraction. Oxygen, nitrogen, strontium, and tantalum atoms are represented as white, black, golden, and blue spheres, respectively. $SrTaO_2N$ has an apparent I4/mcm space group at room temperature because of tilting, but N/O order lowers the tetrago-nal symmetry to Fmmm. (c) N/O order in ABO_2N perovskite oxynitrides showing disordered *cis* N-M-N zig-zag chains (blue line) confined in planes.[11]

Highly sintered ceramics of this perovskite cannot be obtained because it decomposes completely at $1100\,^{\circ}C$ under N_2 into a mix-ture of $LaTiO_3$, La_2O_3, and TiN.[41] Using DFT calculations, spon-taneous polarization has been predicted in thin films, induced by epitaxial strain on the anion order.[42]

The compounds $LnTiO_2N$ with Ln = Nd, Ce, Pr,[43,44] and Eu[45] have also been also investigated for their photocatalytic and electronic properties. The four oxynitrides show the orthorhom-bic $GdFeO_3$-type structure with tilting system $a^+b^-b^-$ and space group Pnma, with a disordered distribution of nitride and oxide.[22,43] In the Ce and Pr compounds, short range anion order has been suggested from electron diffraction experiments. $NdTiO_2N$, $CeTiO_2N$, and $PrTiO_2N$ show bandgaps in the range of 2.0–2.1 eV, close to $LaTiO_2N$. The photocatalytic activity in water oxidation of $NdTiO_2N$ in the presence of a sacrificial agent is similar to that of the lanthanum compound. However, the Pr and Ce compounds show lower activities, which is ascribed to the presence of localized f-orbital states in the bandgap or near the valence band maximum that act as electron–hole recombi-nation centers.[44] $EuTiO_2N$ can be prepared from the oxyhydride $EuTiO_{2.82}H_{0.18}$ by H^-/N^{3-} exchange under NH_3.[45] Magnetic mea-surements indicate that in this oxynitride europium shows the oxi-dation state +3, in contrast with perovskites of other early transi-tion metals such as $Eu^{+2}TaO_2N$, $Eu^{+2}NbO_2N$,[6] and $Eu^{+2}WON_2$.[46] A similar H^-/N^{3-} topochemical exchange synthetic approach has been used to introduce nitride in the perovskites $BaTiO_3$
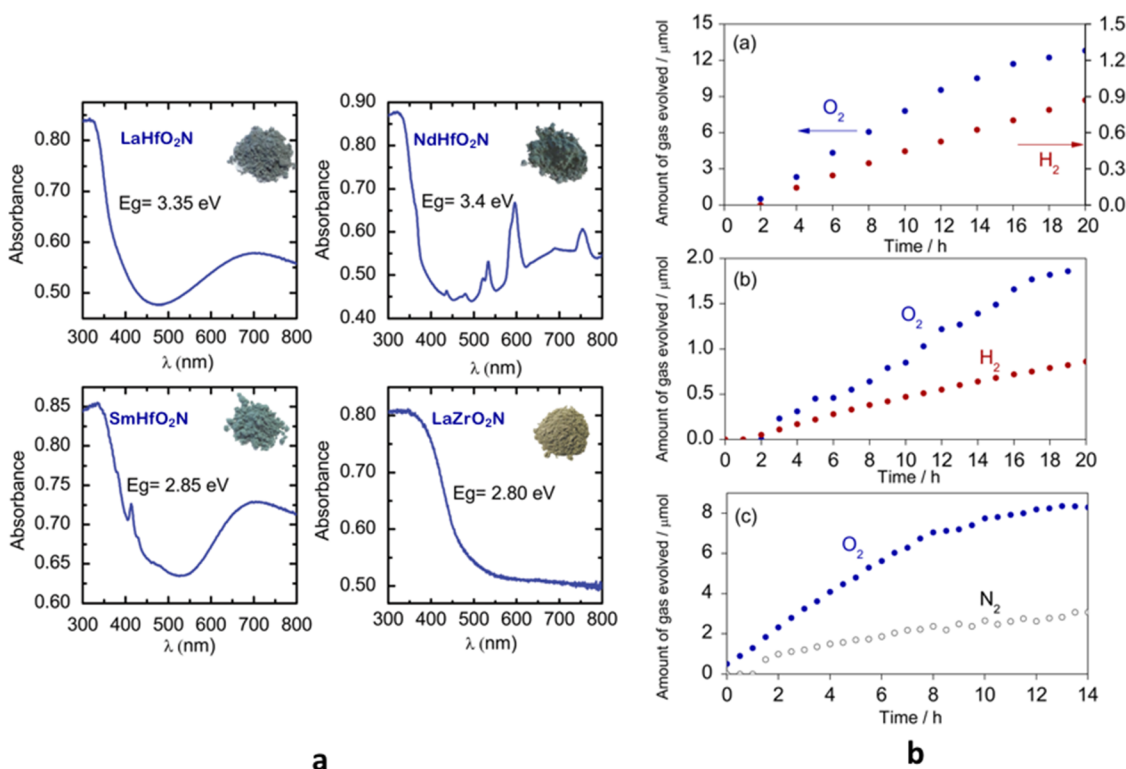
FIG. 2. (a) Diffuse reflectance spectra, bandgaps determined using the Kubelka–Munk function, and powder photographs of $LaHfO_2N$, $NdHfO_2N$, $SmHfO_2N$, and $LaZrO_2N$.[49] (b) Time courses of H_2 or O_2 evolution from aqueous methanol solution or aqueous $AgNO_3$ solution, respectively, on (a) $LaHfO_2N$, (b) $NdHfO_2N$, and (c) $LaZrO_2N$ sample under light irradiation ($\lambda > 300$ nm for $LnHfO_2N$ samples or $\lambda > 400$ nm for $LaZrO_2N$). (a) and (b) are adapted and reproduced with permission from Black et al., Chem. Commun. **54**, 1525 (2018). Copyright 2018 Royal Society of Chemistry.

and $SrTiO_3$.[7] Ferroelectric $BaTiO_{2.4}N_{0.4}$ has been prepared by ammonolysis of $BaTiO_{3-x}H_x$, and oxy-hydride-nitrides have been obtained as intermediate products starting either with $BaTiO_{3-x}H_x$ or $SrTiO_{3-x}H_x$.

B. Zirconium and hafnium

$LaZrO_2N$ was prepared for the first time by ammonolysis of amorphous $La_2Zr_2O_7$ during several weeks at 950 °C.[22] The same perovskite has been more recently synthesized in N_2 by reaction between La_2O_3, ZrN, and ZrO_2 at 1500 °C during 25 h.[47] Zirconium perovskites of smaller rare earths such as Pr, Nd, and Sm could not be prepared by similar synthesis methods, but they can be accessed under 2–3 GPa pressure at 1200–1500 °C starting with a mixture of Zr_2N_2O and Ln_2O_3.[48] All zirconium rare earth perovskites adopt the distorted $GdFeO_3$-type structure, and a total disorder of anions has been reported for $LaZrO_2N$. The isostructural $LnHfO_2N$ compounds with Ln = La, Pr, and Sm are prepared at room pressure at 1500 °C treating a mixture of Hf_2N_2O and Ln_2O_3 for 3 h.[47] As reported for $LaZrO_2N$, a totally disordered distribution of N and O has been found from Rietveld refinement of neutron powder diffraction data. $LaZrO_2N$, $LaHfO_2N$, $PrHfO_2N$, and $SmHfO_2N$ are semiconductors with bandgaps of 2.80 eV, 3.35 eV, 3.40 eV,

and 2.85 eV, respectively, determined from diffuse reflectance spectroscopy [Fig. 2(a)].[49] These are reduced by 2 eV or more with respect to the oxidic perovskites $SrHfO_3$, $BaHfO_3$, or $BaZrO_3$ that show bandgaps of 5.7 eV, 5.8 eV, and 5 eV, respectively, and are larger by 0.7 eV or more as compared to $LaTiO_2N$. The bandgap increase in $LnBO_2N$ (Ln = lanthanide) perovskites within the 4 group of transition metals from 3d to 5d row is due to the increased potential of the empty d orbitals that mainly contribute to the conduction bands. The Zr and Hf compounds show photocatalytic activity in water oxidation or reduction in the presence of co-catalysts. $LaHfO_2N$ and $NdHfO_2N$ have adequate reduction and oxidation potentials to perform the overall water splitting reaction, and $LaZrO_2N$ has the ability to oxidize water under visible light although it undergoes self-oxidative decomposition evolving N_2[47] [Fig. 2(b)]. In contrast with $LaTiO_2N$, the measured dielectric constants of zirconium and hafnium perovskite oxynitrides are relatively low. At room temperature, ε_r was 30 for $LaZrO_2N$ and $LaHfO_2N$, 16 for $NdHfO_2N$, and 28 for $SmHfO_2N$ (Fig. 3). These values are similar to those for the oxidic perovskites $BaHfO_3$, $SrHfO_3$, and $CaHfO_3$ ($\varepsilon_r = 24.2, 23.5,$ and 21.4, respectively) and suggest potential applications of these oxynitrides in memory capacitors.[50]
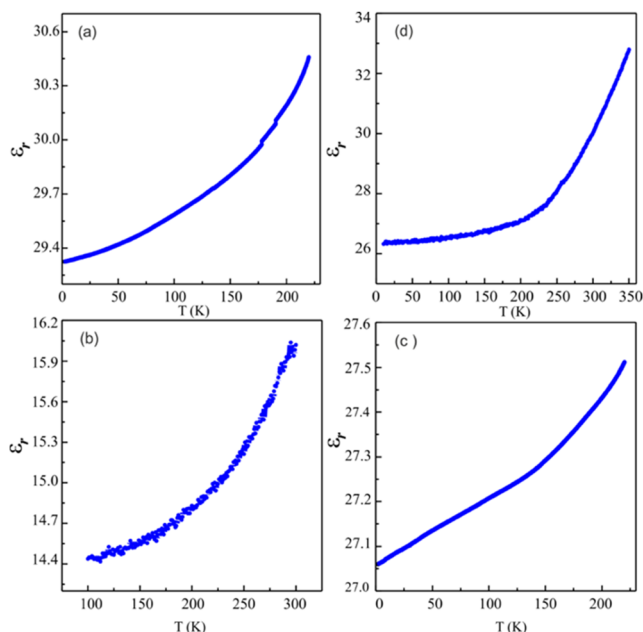
FIG. 3. Temperature dependence of dielectric permittivities of (a) $LaHfO_2N$, (b) $NdHfO_2N$, (c) $SmHfO_2N$, and (d) $LaZrO_2N$ measured at 100 kHz. Reproduced with permission from Black *et al.*, Chem. Commun. **54**, 1525 (2018). Copyright 2018 Royal Society of Chemistry.

III. VANADIUM, NIOBIUM, AND TANTALUM COMPOUNDS

A. Vanadium

Vanadium oxynitride perovskites have been investigated for their electrical and magnetic properties. $LaVO_{3-x}N_x$ samples ($0 < x < 0.9$) were first prepared by Marchand *et al.* by treatment of $LaVO_4$ under NH_3,[51] and perovskites of Pr and Nd were further synthesized using a similar synthetic approach.[30,52] The nitridation of $LnVO_4$ compounds proceeds through a first step of reduction to $LaVO_3$ followed by the incorporation of nitride in this perovskite with concomitant oxidation of V^{3+} to V^{4+}. $LnVO_{3-x}N_x$ (Ln = La, Pr, Nd) with x up to 1 show the $GdFeO_3$ type structure at room temperature. $NdVO_2N$ and $PrVO_{2.24}N_{0.76}$ with vanadium in d^1 and d^1/d^2 configurations, respectively, show partial anion order consistent with *cis*-VN_2 chains similarly to perovskite oxynitrides of d^0 transition metals, indicating that this distribution is robust to electron doping and to the disorder created by non-stoichiometry. $LaVO_{2.09}N_{0.91}$ and $PrVO_{2.24}N_{0.76}$ show spin freezing transitions at low temperatures, and $NdVO_2N$ is paramagnetic. Epitaxial thin films of $LaVO_{3-x}N_x$ have been grown by plasma-assisted pulsed laser deposition.[53] They are highly crystalline and electrically insulating which is suggested to be a consequence of carrier localization induced by anion disorder.

B. Niobium and Tantalum

1. Synthesis

Tantalum and niobium perovskites are extensively investigated for their dielectric properties or their photocatalytic activity in water

splitting among other chemical reactions. Alkaline earth oxynitride perovskites were initially prepared by solid state reaction between the carbonates of calcium, strontium, or barium and Nb_2O_5 or Ta_2O_5 at 950–1000 °C under gaseous ammonia.[15] Alternative synthetic approaches have used precursor oxides such as $Ca_2Nb_2O_7$,[3] $Sr_2Nb_2O_7$, or $SrNbO_3$ for treatment at similar temperatures under NH_3[54] or other nitriding agents such as urea.[55] Synthesis under N_2 gas requires higher temperatures, up to 1500 °C, producing highly crystalline materials and sintered ceramics suitable for electrical measurements. $TaON$, Ta_3N_5, or TaN have been used as reagents, mixed with the alkaline earth carbonate or oxide, for the synthesis of $CaTaO_2N$, $SrTaO_2N$, and $BaTaO_2N$.[17,56,57] More recently $SrNbO_2N$ has been prepared in similar conditions, starting with a mixture of NbN and $SrCO_3$.[58] Large crystals, with sizes up to 10 μm, have been obtained for Sr and Ba perovskites by ammonothermal synthesis at 627 °C, starting from Nb or Ta and Sr or Ba metals and using NaN_3 and $NaOH$ as mineralizers.[59] For $BaNbO_2N$, a self propagating high temperature synthesis method has been recently used, starting with $Ba(OH)_2$, $NbCl_5$, and $NaNH_2$. The reaction took place heating at 225 °C,[60] and the thermodynamical driving force was the formation of $NaCl$ together with $BaNbO_2N$. A similar reaction was previously reported for $BaTaO_2N$ at 223 °C although it was not described as explosive.[61] These are the lowest temperatures reported up to now for the synthesis of perovskite oxynitrides.

Rare earth perovskite oxynitrides $LnBON_2$ with Ln = La, Ce, Pr, Nd, Sm and Gd or $EuBO_2N$ (B = Nb, Ta) are generally prepared by treating the scheelites $LnBO_4$ under NH_3 at 950 °C.[6,12,25] Ammonothermal synthesis has also been used, by reacting the metals or their alloys with NaN_3 or $NaNH_2$ and $NaOH$ at pressures of 100–300 MPa.[62–65] This method produces crystals with sizes up to 15 μm.

2. Crystal symmetries and anion order

Some tantalum and niobium oxynitride perovskites look cubic from laboratory x-ray diffraction data, but they show distortions from synchrotron x-ray diffraction, electron diffraction, or neutron diffraction data. $BaTaO_2N$ and $BaNbO_2N$ have only been reported in the ideal cubic structure Pm-3m.[66] Neutron diffraction data of $SrTaO_2N$ and $SrNbO_2N$ are refined using the space group I4/mcm in the superstructure $\sqrt{2}\, a_p \times \sqrt{2}\, a_p \times 2\, a_p$ due to ordered rotations of the octahedra,[17,67,68] and electron diffraction showed symmetry lowering to Fmmm induced by anion order[11,29] (Fig. 1). The observed anion distribution in both compounds is consistent with a *cis* configuration of nitrides stabilized by covalency and the formation of disordered zig-zag N-M-N chains as suggested for other perovskite oxynitrides including cubic $BaTaO_2N$.[69–71] In the $Ba_{1-x}Sr_xTaO_2N$ series, a sharp crossover from two-dimensional to three-dimensional distribution of *cis*-TaN chains occurs for x near 0.2 (Fig. 4).[71]

$CaTaO_2N$ with the $GdFeO_3$ type structure shows N/O distribution similar to $SrTaO_2N$ and $SrNbO_2N$ compounds.[67] Divalent europium compounds $EuTaO_2N$ and $EuNbO_2N$ show structural distortions similar to $SrTaO_2N$ and $SrNbO_2N$,[6] in contrast to the remaining rare earth compounds that show more distorted structures, with different tilting systems and space groups I2/m or Immma for $LaTaON_2$[12,29,67] and Pnma for $LaNbON_2$,[72]
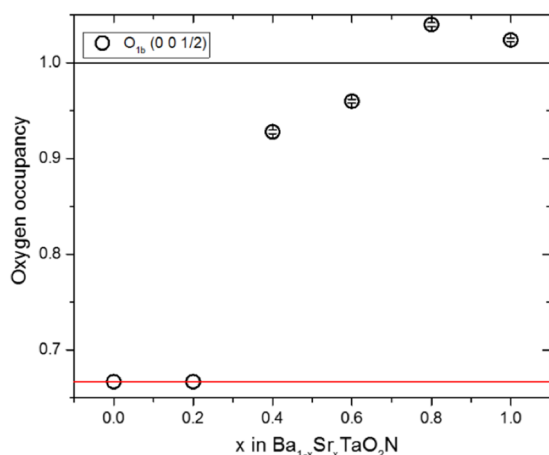
FIG. 4. Plot of oxygen occupancies from room temperature neutron refinements against x in the $Ba_{1-x}Sr_xTaO_2N$ series for the c-axis anion site. Values for the x = 0–0.2 cubic $Pm\bar{3}m$ refinements are fixed at 0.67 which averages over the 3D *cis*-TaN chains. Occupancies for the x = 0.4–1 samples are refined against the tetragonal P4/mmm model which averages the 2D *cis*-TaN chains model. Reproduced with permission from Johnston *et al.*, Chem. Commun. **54**, 5245 (2018). Copyright 2018 Royal Society of Chemistry.

CeTaON$_2$, and PrTaON$_2$.[12] The anion distributions reported for LaTaON$_2$ and LaNbON$_2$ are similar to those found in SrTaO$_2$N, SrNbO$_2$N, LaTiO$_2$N and in vanadium oxynitride perovskites, consistent with a *cis* configuration of nitrides (Fig. 1). Recent DFT studies have shown that anion order has an important effect on the bandgaps and band edge positions of CaTaO$_2$N and SrTaO$_2$N, affecting the photocatalytic activity and other properties.[14,73] Epitaxial strain in thin films of Ca$_{1-x}$Sr$_x$TaO$_2$N has been found to affect the anion order in a recent study performed by a linearly polarized x-ray absorption near-edge structure (XANES) and electron microscopy.[74]

Ruddlesden–Popper[75,76] perovskite oxynitrides (AX)(ABX$_3$)$_n$ (X = N, O) have been reported for tantalum and niobium. n = 1 Sr$_2$TaO$_3$N[77] and Sr$_2$NbO$_3$N, and n = 2 Sr$_3$Nb$_2$O$_5$N$_2$[21] crystallize in space group I4/mmm. For A = rare earth, the only reported examples are n = 2 Eu$_3$Ta$_2$N$_4$O$_3$, which has been recently prepared by ammonothermal synthesis,[78] and the related compound Li$_2$LaTa$_2$O$_6$N,[79] that shows lithium with tetrahedral co-ordination in the AX layers. For n = 1 compounds, neutron diffraction studies show that anions order partially so nitrogen and oxygen occupy the 4c equatorial sites with 50% occupancies, and oxygen prefers the 4e axial positions.[80,81] This order can be rationalized by Pauling's second crystal rule[10,82] because the equatorial sites show larger bond strength sums than the axial ones, and it is also consistent with the local *cis* order of nitrides suggested for pseudocubic perovskites.

3. Photocatalytic properties

Extensive investigation on the photocatalytic activity of tantalum and niobium perovskite oxynitrides in water oxidation and reduction has been developed by Domen's group.[2,34,83] The alkaline earth compounds of Ca, Sr, and Ba show bandgaps between 1.7 eV

(BaNbO$_2$N) and 2.4 eV (CaTaO$_2$N), with corresponding absorption edges between 730 nm and 510 nm, respectively.[84–86] Some of these perovskites have adequate potentials for photocatalytic water oxidation and reduction;[87,88] however, except for CaTaO$_2$N,[89] they cannot achieve the overall water splitting. Recent progress has been made in lanthanum based compounds. The complex oxynitride LaMg$_{1/3}$Ta$_{2/3}$O$_2$N, with a cation disordered double perovskite structure, was first reported by Kim and Woodward.[90] It has been reported as the first example of a overall water splitting photocatalyst active under visible light up to 600 nm[91,92] and the most promising material with respect to its wide range of usable wavelengths. LaTaON$_2$ shows a bandgap of 1.9 eV (absorption edge of 640 nm) and can evolve H$_2$ and O$_2$ from aqueous solution.[93] The H$_2$ evolution activity is weak, but it can be enhanced in core-shell structures obtained by ammonolysis of LaKNaTaO$_5$.[94]

4. Electronic properties

The dielectric properties of tantalum perovskites SrTaO$_2$N and BaTaO$_2$N were initially investigated by Marchand *et al.*[95] and further by Kim *et al.* that reported relative permittivities at room temperatures of 4900 and 2900, respectively.[3] Further measurements performed on dense ceramics led lower values of 450 for SrTaO$_2$N[96] and 320–620 for BaTaO$_2$N.[97] Ferroelectricity in SrTaO$_2$N has been reported for epitaxial thin films[98] and in the surface of sintered ceramics post-annealed in NH$_3$.[8] Both compounds are centrosymmetric, and the origin of their high dielectric constants or ferroelectricity is under discussion although it is generally ascribed to the presence of local electrical dipoles induced by the anion order in the TaO$_4$N$_2$ octahedra.[69,99]

Analogous divalent europium compounds EuTaO$_2$N and EuNbO$_2$N are electrically insulating and show ferromagnetism induced by coupling of europium 7/2 spins.[6] The niobium compound may show slight nitrogen deficiency which induces giant magnetoresistance as a consequence of coupling between the Eu^{2+} spins and the Nb^{4+} carriers.

IV. CHROMIUM, MOLYBDENUM, TUNGSTEN, AND LATER TRANSITION METAL COMPOUNDS

Perovskite oxynitrides of group 6 have been less investigated than for other early transition metals. All of them show nitrogen non-stoichiometry and form solid solutions ABO$_{3-x}$N$_x$ where the transition metal shows mixed valence states of +3/+4 for Cr, +4/+5 or +5/+6 for Mo, and +5/+6 for W. Chromium compounds have only been reported for LnCrO$_{3-x}$N$_x$ with Ln = La, Pr, and Nd and nitrogen contents up to x = 0.59, that have been investigated for their magnetic properties.[100] They are prepared by nitriding LnCrO$_4$ precursors under NH$_3$ for long treatment times and high flow rates. The ammonolysis reaction proceeds similarly to that observed for LnVO$_{3-x}$N$_x$ perovskites, with a first reduction step of LnCrO$_4$ to poorly nitride LnCrO$_{3-x}$N$_x$ compounds with chromium mainly in +3 state, followed by increased incorporation of nitride with concomitant oxidation of Cr^{3+} to Cr^{4+}. LnCrO$_3$ perovskites crystallize in the GdFeO$_3$ type structure and show antiferromagnetic order of Cr^{3+} spins which varies with the size and 4f^n moments of the Ln^{3+} cations.[101] The hole doping trough O^{2-}/N^{3-} anion substitution decreases the Néel temperature but less drastically than for cation substitutions of Ln^{3+} by rare earth cations. The larger covalency of
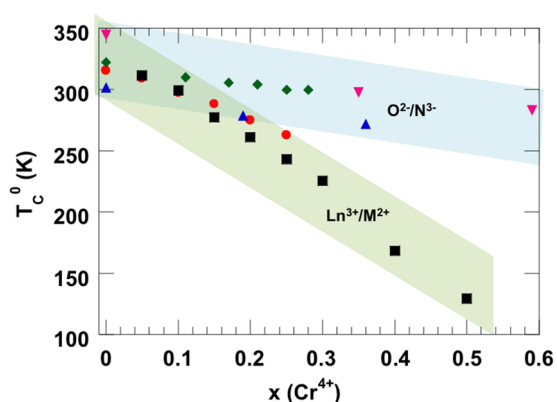
FIG. 5. Cr spin ordering temperatures corrected for lattice effects for doped LnCrO$_3$ materials [LnCrO$_{3-x}$N$_x$ (Ln = La, Pr, Nd), La$_{1-x}$Sr$_x$CrO$_3$, and La$_{1-x}$Ca$_x$CrO$_3$] as a function of Cr^{4+}. Reproduced with permission from Black *et al.*, Chem. Commun. **52**, 4317 (2016). Copyright 2016 Royal Society of Chemistry.

metal-nitride bonds compared to metal-oxide bonds increases the antiferromagnetic interaction between Cr atoms, compensating for the reduction of T$_C$ induced by hole doping (Fig. 5).

Molybdenum and tungsten perovskite oxynitrides have been explored for their magnetic and thermoelectric properties and more recently as photocatalysts in several chemical reactions. Molybdenum compounds have only been reported for strontium in the A sites. The treatment in NH$_3$ at 750–900 °C of SrMoO$_4$ scheelites produces cubic Pm-3m SrMoO$_{3-x}$N$_x$ (0.40 ≤ x ≤ 1.27)[5,20,102,103] perovskites that have been investigated as thermoelectric materials. Tungsten compounds were first reported by Marchand *et al.*, that prepared tetragonal LnWO$_{3-x}$N$_x$ perovskites (Ln = La, Nd; x = 2.2, 2.3, 2.4)[104] by treatment of Ln$_2$W$_2$O$_9$ in ammonia at temperatures between 700 °C and 900 °C. These compounds have been recently prepared as thin films[105] by radiofrequency reactive sputtering, using elemental La and W targets and Si substrates. SrWO$_2$N[106]

can be prepared in similar conditions to SrMoO$_{3-x}$N$_x$. It shows high stability as photocatalyst in oxygen evolution under visible light, in contrast to the lanthanide perovskites LnWO$_{3-x}$N$_x$ (Ln = La, Pr, Nd, Eu) that evolve N$_2$.[107] Highly porous LaWO$_{3-x}$N$_x$ has been recently reported as a photoelectrocatalyst for water splitting under infrared light, at wavelengths above 780 nm.[108] Pseudocubic EuWO$_{1+x}$N$_{2-x}$ compounds are prepared by ammonolysis of Eu$_2$W$_2$O$_9$ with N contents tuned by the ammonia flow rate and temperature.[46] They may show europium in +2/+3 oxidation states and tungsten in +5/+6 oxidation states, which leads to different electrical and magnetic properties as a function of the N/O ratio. They order ferromagnetically at 12 K, and colossal magnetoresistances at low temperatures are observed for the least doped sample (x = −0.04).

Double perovskite oxynitrides of tungsten or molybdenum and iron are prepared by topochemical nitridation of the corresponding cation ordered oxides. The ammonolysis of Sr$_2$FeWO$_6$ at temperatures between 600 °C and 660 °C produces new antiferromagnetic Sr$_2$FeWO$_{6-x}$N$_x$ compounds that keep the cation order of the precursor oxide, with 0 < x ≤ 1, and Néel temperatures between 37 K and 13 K.[109] A similar synthetic route has been used to investigate the effect of nitride on Sr$_2$FeMoO$_6$, an important material that shows metallic conductivity, ferromagnetism, and magnetoresistance at room temperature. The topochemical nitridation of this oxide leads the cation ordered double perovskite oxynitride Sr$_2$FeMoO$_{4.9}$N$_{1.1}$ that is ferromagnetic with T$_c$ ≈ 100 K and also shows negative magnetoresistance.[110] The two oxynitrides Sr$_2$FeWO$_5$N and Sr$_2$FeMoO$_{4.9}$N$_{1.1}$ show superstructures of the perovskite subcell with parameters $\sqrt{2}$ a$_p$ × $\sqrt{2}$ a$_p$ × 2 a$_p$ and 2 a$_p$ × 2 a$_p$ × 2 a$_p$, respectively. The tolerance factor increases with nitriding as a consequence of the oxidation of the B cations (Fe^{2+} to Fe^{3+}and Fe^{4+}, and Mo^{5+} to Mo^{6+}), inducing symmetry increasing, from P2$_1$/n for Sr$_2$FeWO$_6$ to I4/m for Sr$_2$FeWO$_5$N and from I4/m for Sr$_2$FeMoO$_6$ to Fm-3m for Sr$_2$FeMoO$_{4.9}$N$_{1.1}$. The introduction of nitride in Sr$_2$FeMoO$_6$ produces changes in the magnetic structure related to the lowering of the Fermi level associated with the oxidation of iron and to carrier localization induced by anion disorder (Fig. 6).
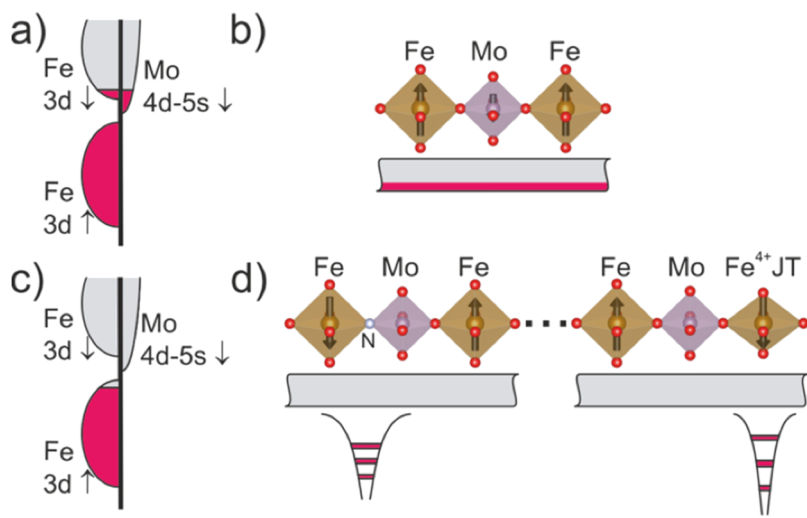

FIG. 6. [(a) and (b)] Schematic band filing of Sr$_2$FeMoO$_6$ and [(c) and (d)] Sr$_2$FeMoO$_{4.9}$N$_{1.1}$. In (d), localized states are formed around defect-related potential wells (e.g., nitride sites, Jahn-Teller Fe^{4+} ions) that trap electrons, hindering carrier mobility, weakening double exchange ferromagnetic interactions, and canceling long range ordering. Reproduced with permission from Ceravola *et al.*, Chem. Commun. **55**, 3105 (2019). Copyright 2019 Royal Society of Chemistry.

V. CONCLUSIONS AND PROSPECTS

Research on transition metal perovskite oxynitrides has progressed substantially in the last years, triggered by important applications that promoted the search of new compounds and the development of synthetic methods. Intensive explorative work of new photocatalysts in water splitting has been performed, leading to the recent discovery of notable materials such as $LaMg_{1/3}Ta_{2/3}O_2N$, a double perovskite oxynitride with low cation order that shows a wide range of usable wavelengths. New hybrid photocatalysts of perovskite oxynitrides active under visible light have been developed for other important chemical reactions such as CO_2 reduction.[111] In the field of electronic materials, ferroelectricity has recently been observed, induced by N/O order, and efforts to produce sintered ceramics have led to improved processing strategies.[112] These include a high pressure/high temperature treatment performed under N_2 to obtain dense ceramics, followed by a simple ammonolysis step for recovering the nitrogen loss that happens at high temperatures and is inherent to some oxynitrides. New strategies for producing dense single crystal thin films with control of anion order have been developed[74] with direct evaluation of N/O distribution through STEM-EELS.

Reported layered perovskite oxynitrides are scarce; however, they show potential tunability of bandgaps and electronic states of the transition metals and are candidates for searching new materials. Oxidic double perovskites $A_2B'B''O_6$[113] show a large diversity of properties as a result of the combination of two different transition metals. Double perovskite oxynitrides $A_2B'B''O_{6-x}N_x$ have been reported for few transition metals and represent another source of new materials. Late transition metals such as iron have been stabilized in perovskite oxynitrides by using adequate precursors for ammonolysis reactions at lower temperatures. Efforts in the development of synthetic strategies should lead to the discovery of important materials in these and other unexplored groups of compounds.

ACKNOWLEDGMENTS

REFERENCES

[1] A. Fuertes, Dalton Trans. **39**, 5942 (2010).
[2] T. Takata and K. Domen, ACS Energy Lett. **4**, 542 (2019).
[3] Y. Kim, P. M. Woodward, K. Z. Baba-Kishi, and C. W. Tai, Chem. Mater. **16**, 1267 (2004).
[4] M. Jansen and H. P. Letschert, Nature **404**, 980 (2000).
[5] D. Logvinovich, R. Aguiar, R. Robert, M. Trottmann, S. G. Ebbinghaus, A. Reller, and A. Weidenkaff, J. Solid State Chem. **180**, 2649 (2007).
[6] A. B. Jorge, J. Oró-Sole, A. M. Bea, N. Mufti, T. T. M. Palstra, J. A. Rodgers, J. P. Attfield, and A. Fuertes, J. Am. Chem. Soc. **130**, 12572 (2008).
[7] T. Yajima, F. Takeiri, K. Aidzu, H. Akamatsu, K. Fujita, W. Yoshimune, M. Ohkura, S. Lei, V. Gopalan, K. Tanaka, C. M. Brown, M. A. Green, T. Yamamoto, Y. Kobayashi, and H. Kageyama, Nat. Chem. **7**, 1017 (2015).
[8] S. Kikkawa, S. Sun, Y. Masubuchi, Y. Nagamine, and T. Shibahara, Chem. Matter **28**, 1312 (2016).
[9] R. Asahi, T. Morikawa, T. Ohwaki, K. Aoki, and Y. Taga, Science **293**, 269 (2001).
[10] A. Fuertes, Inorg. Chem. **45**, 9640 (2006).
[11] M. Yang, J. Oró-Solé, J. A. Rodgers, A. B. Jorge, A. Fuertes, and J. P. Attfield, Nat. Chem. **3**, 47 (2011).
[12] S. H. Porter, Z. Huang, and P. M. Woodward, Cryst. Growth Des. **14**, 117 (2014).
[13] J. P. Attfield, Cryst. Growth Des. **13**, 4623 (2013).
[14] A. Ziani, C. Le Paven, L. Le Gendre, F. Marlec, R. Benzerga, F. Tessier, F. Cheviré, M. N. Hedhili, A. T. Garcia-Esparza, S. Melissen, P. Sautet, T. Le Bahers, and K. Takanabe, Chem. Matter **29**, 3989 (2017).
[15] R. Marchand, F. Pors, and Y. Laurent, Rev. Int. Hautes Temp. Refract. **23**, 11 (1986).
[16] A. Fuertes, Prog. Solid State Chem. **51**, 63 (2018).
[17] S. J. Clarke, K. A. Hardstone, C. W. Michie, and M. J. Rosseinsky, Chem. Mater. **14**, 2664 (2002).
[18] R. Marchand, C. R. Acad. Sci. Paris **282**, 329 (1976).
[19] R. Marchand and Y. Laurent, Patent CNRS-ANVAR 84-17274 (13 November 1984).
[20] G. Liu, X. Zhao, and H. A. Eick, J. Alloys Compd. **187**, 145 (1992).
[21] G. Tobías, J. Oró-Solé, D. Beltrán-Porter, and A. Fuertes, Inorg. Chem. **40**, 6867 (2001).
[22] S. J. Clarke, B. P. Guinot, C. W. Michie, M. J. C. Calmont, and M. J. Rosseinsky, Chem. Mater. **14**, 288 (2002).
[23] S. G. Ebbinghaus, H.-P. Abicht, R. Dronskowski, T. Müller, A. Reller, and A. Weidenkaff, Prog. Solid State Chem. **37**, 173 (2009).
[24] A. Fuertes, J. Mater. Chem. **22**, 3293 (2012).
[25] R. Marchand, F. Pors, and Y. Laurent, Ann. Chim. **16**, 553 (1991).
[26] R. Okada, K. Katagiri, Y. Masubuchi, and K. Inumaru, Eur. J. Inorg. Chem. **2019**, 1257.
[27] M. Yashima, M. Saito, H. Nakano, T. Takata, K. Ogisu, and K. Domen, Chem. Commun. **46**, 4704 (2010).
[28] D. Habu, Y. Masubuchi, S. Torii, T. Kamiyama, and S. Kikkawa, J. Solid State Chem. **237**, 254 (2016).
[29] L. Clark, J. Oró-Solé, K. S. Knight, A. Fuertes, and J. P. Attfield, Chem. Mater. **25**, 5004 (2013).
[30] J. Oró-Solé, L. Clark, W. Bonin, J. P. Attfield, and A. Fuertes, Chem. Commun. **49**, 2430 (2013).
[31] S. Ninova and U. Aschauer, J. Mater. Chem. A **7**, 2129 (2019).
[32] A. Kasahara, K. Nukumizu, G. Hitoki, T. Takata, J. N. Kondo, M. Hara, H. Kobayashi, and K. Domen, J. Phys. Chem. A **106**, 6750 (2002).
[33] C. Le Paven-Thivet, A. Ishikawa, A. Ziani, L. Le Gendre, M. Yoshida, J. Kubota, F. Tessier, and K. Domen, J. Phys. Chem. C **113**, 6156 (2009).
[34] C. M. Leroy, A. E. Maegli, K. Sivula, T. Hisatomi, N. Xanthopoulos, E. H. Otal, S. Yoon, A. Weidenkaff, R. Sanjines, and M. Grätzel, Chem. Commun. **48**, 820 (2012).
[35] F. Zhang, A. Yamakata, K. Maeda, Y. Moriya, T. Takata, J. Kubota, K. Teshima, S. Oishi, and K. Domen, J. Am. Chem. Soc. **134**, 8348 (2012).
[36] T. Hisatomi and K. Domen, Nat. Catal. **2**, 387 (2019).
[37] M. Hojamberdiev, A. Yamaguchi, K. Yubuta, S. Oishi, and K. Teshima, Inorg. Chem. **54**, 3237 (2015).
[38] L. Lu, B. Wang, S. Wang, Z. Shi, S. Yan, and Z. Zou, Adv. Funct. Mater. **27**, 1702447 (2017).
[39] D. Fasquelle, A. Ziani, C. Le Paven-Thivet, L. Le Gendre, and J. C. Carru, Matter Lett. **65**, 3102 (2011).
[40] Y. Lu, C. Le Paven, H. V. Nguyen, R. Benzerga, L. Le Gendre, S. Rioual, F. Tessier, F. Cheviré, A. Sharaiha, C. Delaveaud, and X. Castel, Cryst. Growth Des. **13**, 4852 (2013).
[41] D. Chen, D. Habu, Y. Masubuchi, S. Torii, and T. Kamiyama, Solid State Sci. **54**, 2 (2016).
[42] N. Vonrüti and U. Aschauer, Phys. Rev. Lett. **120**, 046001 (2018).
[43] S. H. Porter, Z. Huang, Z. Heng, M. Avdeev, Z. Chen, S. Dou, and P. M. Woodward, J. Solid State Chem. **226**, 279 (2015).
[44] S. H. Porter, Z. Huang, S. Dou, S. Brown-Xu, A. T. M. G. Sarwar, R. C. Myers, and P. M. Woodward, Chem. Matter **27**, 2414 (2015).

[45] R. Mikita, T. Aharen, T. Yamamoto, F. Takeiri, T. Ya, W. Yoshimune, K. Fujita, S. Yoshida, K. Tanaka, D. Batuk, A. M. Abakumov, C. M. Brown, Y. Kobayashi, and H. Kageyama, J. Am. Chem. Soc. **138**, 3211 (2016).

[46] M. Yang, J. Oró-Solé, A. Kusmartseva, A. Fuertes, and J. P. Attfield, J. Am. Chem. Soc. **132**, 4822 (2010).

[47] A. P. Black, H. Suzuki, M. Higashi, C. Frontera, C. Ritter, C. De, A. Sundaresan, R. Abe, and A. Fuertes, Chem. Commun. **54**, 1525 (2018).

[48] M. Yang, J. A. Rodgers, L. C. Middler, J. Oró-Solé, A. B. Jorge, A. Fuertes, and J. P. Attfield, Inorg. Chem. **48**, 11498 (2009).

[49] A. P. Black, Ph.D. thesis, Autonomous University of Barcelona, 2017.

[50] A. Feteira, D. C. Sinclair, K. Z. Rajab, and M. T. Lanagan, J. Am. Ceram. Soc. **91**, 893 (2008).

[51] P. Antoine, R. Assaba, P. L'Haridon, R. Marchand, Y. Laurent, C. Michel, and B. Raveau, Mater. Sci. Eng.: B **5**, 43 (1989).

[52] J. Oró-Solé, L. Clark, N. Kumar, W. Bonin, A. Sundaresan, J. P. Attfield, C. N. Rao, and A. Fuertes, J. Mater. Chem. C **2**, 2212 (2014).

[53] M. Sano, Y. Hirose, S. Nakao, and T. Hasegawa, J. Mater. Chem. C **5**, 1798 (2017).

[54] M. Kodera, Y. Moriya, M. Katayama, T. Hisatomi, T. Minegishi, and K. Domen, Sci. Rep. **8**, 15849 (2018).

[55] A. Gomathi, S. Reshma, and C. N. R. Rao, J. Solid State Chem. **182**, 72 (2009).

[56] S.-K. Sun, T. Motohashi, Y. Masubuchi, and S. Kikkawa, J. Eur. Ceram. Soc. **34**, 4451 (2014).

[57] S.-K. Sun, Y. Masubuchi, T. Motohashi, and S. Kikkawa, J. Eur. Ceram. Soc. **35**, 3289 (2015).

[58] W.-B. Niu, S.-K. Sun, W.-M. Guo, S.-L. Chen, M. Lv, H.-T. Lin, and C.-Y. Wang, Ceram. Int. **44**, 23324 (2018).

[59] N. Cordes, T. Bräuniger, and W. Schnick, Eur. J. Inorg. Chem. **2018**, 5019.

[60] J. Odahara, A. Miura, N. C. Rosero-Navarro, and K. Tadanaga, Inorg. Chem. **57**, 24 (2018).

[61] Y. Setsuda, Y. Maruyama, C. Izawa, and T. Watanabe, Chem. Lett. **46**, 987 (2017).

[62] T. Watanabe, K. Tajima, J. W. Li, N. Matsushita, and M. Yoshimura, Chem. Lett. **40**, 1101 (2011).

[63] C. Izawa, T. Kobayashi, K. Kishida, and T. Watanabe, Adv. Mat. Sci. Eng. **2014**, 465720.

[64] N. Cordes and W. Schnick, Chem. - Eur. J. **23**, 11410 (2017).

[65] J. Häusler and W. Schnick, Chem. - Eur. J. **24**, 11864 (2018).

[66] F. Pors, R. Marchand, and Y. Laurent, Mater. Res. Bull. **23**, 1447 (1988).

[67] E. Gunther, R. Hagenmayer, and M. Jansen, Z. Anorg. Allg. Chem. **626**, 1519 (2000).

[68] S. G. Ebbinghaus, A. Weidenkaff, A. Rachel, and A. Reller, Acta Crystallogr., Sect. C: Cryst. Struct. Commun. **60**, i91 (2004).

[69] K. Page, M. W. Stoltzfus, Y.-I. Kim, T. Proffen, P. M. Woodward, A. K. Cheetham, and R. Seshadri, Chem. Mater. **19**, 4037 (2007).

[70] H. Wolff and R. Dronskowski, J. Comput. Chem. **29**, 2260 (2008).

[71] H. Johnston, A. P. Black, P. Kayser, J. Oró-Solé, D. A. Keen, A. Fuertes, and J. P. Attfield, Chem. Commun. **54**, 5245 (2018).

[72] D. Logvinovich, S. G. Ebbinghauss, A. Reller, I. Marozau, D. Ferri, and A. Weidenkaff, Z. Anorg. Allg. Chem. **636**, 905 (2010).

[73] A. Kubo, G. Giorgi, and K. Yamashita, Chem. Mater. **29**, 539 (2017).

[74] D. Oka, Y. Hirose, F. Matsui, H. Kamisaka, T. Oguchi, N. Maejima, H. Nishikawa, T. Muro, K. Hayashi, and T. Hasegawa, ACS Nano **11**, 3860 (2017).

[75] S. N. Ruddlesden and P. Popper, Acta Crystallogr. **10**, 538 (1957).

[76] S. N. Ruddlesden and P. Popper, Acta Crystallogr. **11**, 54 (1958).

[77] F. Pors, R. Marchand, and Y. Laurent, Ann. Chim. **16**, 547 (1991).

[78] N. Cordes, M. Nentwig, L. Eisenburger, O. Oeckler, and W. Schnick, Eur. J. Inorg. Chem. **2019**, 2304.

[79] M. Kaga, H. Kurachi, T. Asaka, B. Yue, J. Ye, and K. Fukuda, Powder Diffr. **26**, 4 (2011).

[80] N. Diot, R. Marchand, J. Haines, J. M. Léger, P. Macaudière, and S. Hull, J. Solid State Chem. **146**, 390 (1999).

[81] G. Tobías, D. Beltrán-Porter, O. Lebedev, G. Van Tendeloo, J. Oró-Solé, J. Rodríguez-Carvajal, and A. Fuertes, Inorg. Chem. **43**, 8010 (2004).

[82] L. Pauling, J. Am. Chem. Soc. **51**, 1010 (1929).

[83] T. Takata, C. Pan, and K. Domen, ChemElectroChem **3**, 31 (2016).

[84] I. E. Castelli, T. Olsen, S. Datta, D. D. Landis, S. Dahl, K. S. Thyegesen, and K. W. Jacobsen, Energy Environ. Sci. **5**, 5814 (2012).

[85] Y. Wu, P. Lazic, G. Hautier, K. Persson, and G. Ceder, Energy Environ. Sci. **6**, 157 (2013).

[86] S. Balaz, S. H. Porter, P. M. Woodward, and L. J. Brillson, Chem. Mater. **25**, 3337 (2013).

[87] K. Maeda, D. Lu, and K. Domen, Angew. Chem., Int. Ed. **52**, 6488 (2013).

[88] J. Seo, T. Hisatomi, M. Nakabayashi, N. Shibata, T. Minegishi, M. Katayama, and K. Domen, Adv. Energy Mater. **8**, 1800094 (2018).

[89] J. Xu, C. Pan, T. Takata, and K. Domen, Chem. Commun. **51**, 7191 (2015).

[90] Y.-I. Kim and P. M. Woodward, J. Solid State Chem. **180**, 3224 (2007).

[91] C. Pan, T. Takata, M. Nakabayashi, T. Matsumoto, N. Shibata, Y. Ikuhara, and K. Domen, Angew. Chem., Int. Ed. **54**, 2955 (2015).

[92] C. Pan, T. Takata, and K. Domen, Chem. - Eur. J. **22**, 1854 (2016).

[93] L. Zhang, Y. Song, J. Feng, T. Fang, Y. Zhong, Z. Li, and Z. Zou, Int. J. Hydrogen Energy **39**, 7697 (2014).

[94] X. Wang, T. Hisatomi, Z. Wang, J. Song, J. Qu, T. Takata, and K. Domen, Angew. Chem., Int. Ed. **58**, 10666 (2019).

[95] R. Marchand, F. Pors, Y. Laurent, O. Regreny, J. Lostec, and J. M. Haussone, J. Phys. **47**(C1), 901 (1986).

[96] S.-K. Sun, Y.-R. Zhang, Y. Masubuchi, T. Motohashi, and S. Kikkawa, J. Am. Ceram. Soc. **97**, 1023 (2014).

[97] A. Hosono, S.-K. Sun, Y. Masubuchi, and S. Kikkawa, J. Eur. Ceram. Soc. **36**, 3341 (2016).

[98] D. Oka, Y. Hirose, H. Kamisaka, T. Fukumura, K. Sasa, S. Ishii, H. Matsuzaki, Y. Sato, Y. Ikuhara, and T. Hasegawa, Sci. Rep. **4**, 4987 (2014).

[99] R. L. Withers, Y. Liu, P. Woodward, and Y.-I. Kim, Appl. Phys. Lett. **92**, 102907 (2008).

[100] A. P. Black, H. E. Johnston, J. Oró-Solé, B. Bozzo, C. Ritter, C. Frontera, J. P. Attfield, and A. Fuertes, Chem. Commun. **52**, 4317 (2016).

[101] R. M. Hornreich, J. Magn. Magn. Mater. **7**, 280 (1978).

[102] D. Logvinovich, J. Hejtmánek, K. Knížek, M. Maryško, N. Homazava, P. Tomès, R. Aguiar, S. G. Ebbinghaus, A. Reller, and A. Weidenkaff, J. Appl. Phys. **105**, 023522 (2009).

[103] W. Li, D. Li, X. Gao, A. Gurlo, S. Zander, P. Jones, A. Navrotsky, Z. Shen, R. Riedel, and E. Ionescu, Dalton Trans. **44**, 8238 (2015).

[104] P. Antoine, R. Marchand, Y. Laurent, C. Michel, and B. Raveau, Mater. Res. Bull. **23**, 953 (1988).

[105] K. R. Talley, J. Magnum, C. L. Perkins, R. Woods-Robinson, A. Mehta, B. P. Gormn, G. L. Brennecka, and A. Zakutayev, Adv. Electron. Mater. **5**, 1900214 (2019).

[106] I. D. Fawcett, K. V. Ramanujachary, and M. Greenblatt, Mater. Res. Bull. **32**, 1565 (1997).

[107] K. Kawashima, M. Hojamberdiev, H. Wagata, E. Zahedi, K. Yubuta, K. Domen, and K. Teshima, J. Catal. **344**, 29 (2016).

[108] K. Kawasima, Y. Liu, J.-H. Kim, B. R. Wygat, I. Cheng, H. Celio, O. Mabayoje, J. Lin, and C. B. Mullins, ACS Appl. Energy Mater. **2**, 913 (2019).

[109] R. Ceravola, J. Oró-Solé, A. P. Black, C. Ritter, I. Puente Orench, I. Mata, E. Molins, C. Frontera, and A. Fuertes, Dalton Trans. **46**, 5128 (2017).

[110] R. Ceravola, C. Frontera, J. Oró-Solé, A. P. Black, C. Ritter, I. Mata, E. Molins, J. Fontcuberta, and A. Fuertes, Chem. Commun. **55**, 3105 (2019).

[111] K. Maeda, Prog. Solid State Chem. **51**, 52 (2018).

[112] Y. Masubuchi, S.-K. Sun, and S. Kikkawa, Dalton Trans. **44**, 10570 (2015).

[113] S. Vasala and M. Karppinen, Prog. Solid State Chem. **43**, 1 (2015).